Parametric entrainment control of chaotic systems

Robert Mettin,* Alfred Hübler, and Alexander Scheeline
Center for Complex Systems Research, Beckman Institute, 405 North Mathews Avenue, University of Illinois at Urbana-Champaign, Urbana, Illinois 61801

Werner Lauterborn
Drittes Physikalisches Institut, Universität Göttingen, Bürgerstraße 42–44, D-37073 Göttingen, Germany
(Received 18 April 1994)

We apply a generalized approach for model-based nonfeedback control to chaotic systems where parametric dependence on the control forces is included. The existing formalism is extended for our purpose. For chaotic iterated maps and ordinary differential equations, we obtain entrainment to stationary, periodic, and aperiodic goal dynamics. Applicability to general resonance spectroscopy is demonstrated.

PACS number(s): 05.45.+b, 06.70.Td, 82.40.Bj

I. INTRODUCTION

Recently, much attention has been paid to methods that intend control of chaotic systems. The aims of control include the elimination of turbulencelike, only short-term predictable behavior in cases where it occurs over a large parameter range (e.g., certain chemical reactions, mechanical vibrations, or fluid flows), easy switching between different solutions embedded in chaotic attractors, and enhancing chaos for several purposes (e.g., dissipation, mixing, or improved system modeling). The proposed methods comprise feedback and nonfeedback techniques. This article addresses the extension of the nonfeedback method known as entrainment control to parametric control forces.

A large number of *feedback* control methods for application to chaotic systems has been introduced so far. They include stochastic control techniques [1], repeated shifts of the system onto stable manifolds of unstable periodic orbits [2–7], switching or proportional feedback control that is applied occasionally [8–13] or continuously [14–16], and proportional-plus-integral control [17–19]. Also, targeting controls including feedback [20–22] have been proposed, and several feedback techniques for spatially extended systems are under consideration [23–26]. Typically, systems that are controlled with one of the above feedback methods settle down on or near an unstable periodic orbit of the (uncontrolled) chaotic system. Therefore in most cases the control forces are small, while the variety of goal dynamics achieved in this way is restricted. In particular, this holds for all adaptive parametric controls introduced so far [27–29] where only natural and stable system dynamics is permitted as a goal. For many feedback techniques, such as the Ott-Grebogi-Yorke (OGY) method [2], no detailed model of the system under control is necessary, though performance can be improved if a global model exists [5].

Nonfeedback control aims at, e.g., applications where none, no real-time, or only highly restricted measurements of the system state are available (e.g., molecule dynamics, certain chemical or biological processes), or where the system behavior is to be altered more drastically. Many publications concern periodic perturbations of nonlinear [30,31] and chaotic systems [32–42]. These works have shown a variety of cases where chaotic motion has been suppressed by periodic perturbations either in parameters or in phase space. Usually, no global model is used to derive exact shapes of control signals (except for derivation of resonant frequencies), and for small control power, the resulting dynamics is close to unstable periodic orbits (similar to most feedback applications).

In contrast to the above perturbation controls, there exist explicitly model-based approaches of open-loop control, first introduced by Hübler and Lüscher [43]. Control forces of this method are completely derived with the help of a global model of the experimental dynamics and a desired goal behavior, to which the system is entrained ("entrainment control"). Further investigations and applications of such controls to chaotic iterated maps [45,49] and ordinary differential equations (ODEs) [44,46–48] show the use for the removal of chaos, but also for other goals (e.g., aperiodic orbits or the transfer between different attractors). The idea of model-based control has also been investigated for reconstructed systems and systems with hidden variables [50,51], noisy systems [52], and partial differential equations [53,54]. In the latter article it is shown that this kind of control also works with low energy cost for goals near the natural system behavior (while more unnatural goal motion, though possible, requires possibly large control forces). The problem of the need for an accurate model equation is addressed in Ref. [55], where the dependence of control performance on modeling parameters is exploited for

*Permanent address: Institut für Angewandte Physik, TH Darmstadt, Schloßgartenstraße 7, D-64289 Darmstadt, Germany.

a general kind of resonance spectroscopy.

All the cited work about model-based entrainment control considers control forces that act additively in phase space. Although the idea of entrainment control via parametric forces has already been stated in Ref. [44], only one work is known to the authors where nonadditive forces really have been used. In Ref. [56], Shermer and Spano employ a model-based derivation of a parametric force to entrain a nonlinear (Duffing-like) oscillator to harmonic motion, both in simulations and experiment. While they obtain excellent results controlling a passive system, the demonstration of the applicability of parametric entrainment control to chaotic dynamics is still lacking.

In this article, we extend the existing theory of entrainment control for the control of chaotic systems on the basis of general control forces. This includes considerations on stability and inaccurate modeling. Using our results, we show nonadditive entrainment control for chaotic iterated maps and ODEs as well as the applicability to general resonance spectroscopy as described in Ref. [55].

In Sec. II we review the main idea of the model-based control method with general forces, as proposed in [44], [56], and add stability considerations necessary for the application to chaotic systems and for general resonance spectroscopy. Examples for parametric control of iterated maps are given in Sec. III; fixed point, periodic, and aperiodic dynamics have been achieved in the one- and two-dimensional cases. Applications of the control method to ODEs are addressed in Sec. IV. Periodic entrainment of the Lorenz system and control of a chemical oscillator model, using restricted control forces, are described. Section V gives a summary and an outlook for further applications and improvements of the control technique.

II. THEORY

The notation in this section corresponds to the dynamics of an iterated map. The generalization to continuous time systems is straightforward and given in Sec. IV.

We assume that the experimental system we want to control can be described by the iterated map

$$\mathbf{x}^{(n+1)} = \mathbf{f}(\mathbf{x}^{(n)}, \mathbf{p}, \mathbf{F}^{(n)}) \quad , \tag{1}$$

where $\mathbf{x}^{(n)} \in \mathbb{R}^d$ denotes the state of the d-dimensional system at time step n, $\mathbf{p} \in \mathbb{R}^k$ a set of k parameters, and $\mathbf{F}^{(n)} \in \mathbb{R}^s$ the control forces at time n. We assume further that we have a global model of the experiment,

$$\mathbf{y}^{(n+1)} = \mathbf{f}(\mathbf{y}^{(n)}, \mathbf{q}, \mathbf{F}^{(n)}) \quad , \tag{2}$$

with $\mathbf{y}^{(n)} \in \mathbb{R}^d, \mathbf{q} \in \mathbb{R}^k$, which has been either derived analytically, or reconstructed from data. Note that the difference between experiment and model is expressed in different parameter vectors, $\mathbf{p}$ and $\mathbf{q}$, respectively. This can always be achieved by a series expansion of both the experimental and the model equations (if both maps are analytic) and adding the expansion coefficients to the parameter vectors (to prevent infinite dimensions, we consider a reasonable truncation of these vectors to finite dimension k). Now we introduce a goal dynamics, i.e., a motion that we want the experiment to do:

$$\mathbf{z}^{(n+1)} = \mathbf{g}(\mathbf{z}^{(n)}), \tag{3}$$

with the goal states $\mathbf{z}^{(n)} \in \mathbb{R}^d$. At this point, there is *a priori* no restriction of our goal. However, stability and other requirements of the control may limit the number of goals that are possible.

To achieve the desired dynamics in our experimental system, we have to choose the control forces $\mathbf{F}^{(n)}$ in such a manner that

$$\mathbf{x}^{(n+1)} = \mathbf{f}(\mathbf{x}^{(n)}, \mathbf{p}, \mathbf{F}^{(n)}) = \mathbf{g}(\mathbf{x}^{(n)}). \tag{4}$$

However, this would require a measurement of $\mathbf{x}^{(n)}$ at each time step to evaluate $\mathbf{f}$ and $\mathbf{g}$ correctly. We can avoid the necessity of feedback if we assume that the system has reached some known state of the goal, say $\mathbf{z}^{(0)}$, and that control works perfectly. Then all further points $\mathbf{x}^{(n)} = \mathbf{z}^{(n)}$ are determined by $\mathbf{g}$ and $\mathbf{z}^{(0)}$, and we can calculate the control forces without any information from the actual system, using

$$\mathbf{f}(\mathbf{z}^{(n)}, \mathbf{p}, \mathbf{F}^{(n)}) = \mathbf{g}(\mathbf{z}^{(n)}) = \mathbf{z}^{(n+1)}. \tag{5}$$

The important question arises of whether the controlled system shows entrainment,

$$\lim_{n\to\infty} |\mathbf{x}^{(n)} - \mathbf{z}^{(n)}| = 0, \tag{6}$$

when it starts apart from the goal. We will come back to this later.

Our considerations contain one more step. Because we have no access to the "real" experimental equation, we solve our model map (with parameters $\mathbf{q}$) to gain the control signals:

$$\mathbf{f}(\mathbf{z}^{(n)}, \mathbf{q}, \mathbf{F}^{(n)}) = \mathbf{g}(\mathbf{z}^{(n)}) = \mathbf{z}^{(n+1)}. \tag{7}$$

In this way, the possibility of control usually deteriorates, but does not break down immediately. Although the exact goal dynamics is no longer a solution of the controlled equation (1) if $\mathbf{p} \neq \mathbf{q}$, the system can be entrained to a similar dynamics for sufficiently good approximations of the true parameters. Control can still be successful, but in a looser sense than given by Eq. (6). To characterize the quality of control if no real convergence towards the goal occurs, one can introduce some measure of similarity, e.g., the limit in Eq. (6) can be replaced by a supremum or a mean over a long time which should be smaller than some finite ϵ. In the following, we extend "entrainment" in the sense that the controlled system follows the goal dynamics within an averaged distance that is small compared to the phase space extension covered by the uncontrolled orbit:

$$\langle \|\mathbf{x}_{con}^{(n)} - \mathbf{z}^{(n)}\| \rangle < \epsilon \ll \max_{m,n} \{\|\mathbf{x}_{nocon}^{(m)} - \mathbf{x}_{nocon}^{(n)}\|\}. \tag{8}$$

If such "near entrainment" [46] is shown by a controlled system, it can be exploited to improve initial parameter guesses by a "trial and error" control method. This is the main idea of general resonance spectroscopy as proposed in Ref. [55]: Model parameters are changed until the control works "best," e.g., the boundary ϵ in Eq. (8) is as small as possible.

For consideration of stability and systematic deviation (near entrainment) of our goal dynamics, we are interested in the difference between the experimental state and the desired goal state. For small distances to the goal, and for small modeling errors, the following linearization of Eq. (1) is valid:

$$\mathbf{x}^{(n+1)} = \mathbf{f}(\mathbf{z}^{(n)}, \mathbf{q}, \mathbf{F}^{(n)}) + Df_z^{(n)}(\mathbf{x}^{(n)} - \mathbf{z}^{(n)}) + Df_q^{(n)}(\mathbf{p} - \mathbf{q}). \tag{9}$$

The two Jacobi matrices are evaluated at the (known) points $\mathbf{z}^{(n)}$, $\mathbf{q}$, and $\mathbf{F}^{(n)}$:

$$Df_z^{(n)} = \left(\frac{\partial f_i}{\partial z_j}\right)\Big|_{\mathbf{z}^{(n)},\mathbf{q},\mathbf{F}^{(n)}}, \quad i,j = 1,\ldots,d, \tag{10}$$

$$Df_q^{(n)} = \left(\frac{\partial f_i}{\partial q_j}\right)\Big|_{\mathbf{z}^{(n)},\mathbf{q},\mathbf{F}^{(n)}}, \; i = 1,\ldots,d\,;\; j = 1,\ldots,k. \tag{11}$$

Using Eq. (7), the control forces $\mathbf{F}^{(n)}$ are chosen in such a way that

$$\mathbf{x}^{(n+1)} - \mathbf{z}^{(n+1)} = Df_z^{(n)}(\mathbf{x}^{(n)} - \mathbf{z}^{(n)}) + Df_q^{(n)}(\mathbf{p} - \mathbf{q}). \tag{12}$$

Let us briefly review the case of additive control forces in each variable,

$$\mathbf{x}^{(n+1)} = \mathbf{f}(\mathbf{x}^{(n)}, \mathbf{p}, \mathbf{F}^{(n)}) = \tilde{\mathbf{f}}(\mathbf{x}^{(n)}, \mathbf{p}) + \mathbf{F}^{(n)}. \tag{13}$$

Solving Eq. (7) immediately leads to

$$\mathbf{F}^{(n)} = \mathbf{z}^{(n+1)} - \tilde{\mathbf{f}}(\mathbf{z}^{(n)}, \mathbf{q}). \tag{14}$$

Jackson [46] defines the *convergent regions* in phase space by the condition that all nearby orbits converge towards each other. A point $\mathbf{z}$ belongs to a convergent region if all eigenvalues of the Jacobi matrix

$$D\tilde{f}_z = \left(\frac{\partial \tilde{f}_i}{\partial z_j}\right)\Big|_{\mathbf{z},\mathbf{q}}, \quad i,j = 1,\ldots,d \tag{15}$$

have an absolute value less than unity. All goals entirely located within convergent regions turn out to be asymptotically stable. However, statements about size and location of their basins of attraction are more difficult to make (refer to Refs. [45,46,49] for some examples). The situation is slightly different for ODE dynamics (see Sec. IV).

The convergent regions in the additive control case are obviously independent of $\mathbf{F}$ and therefore of the specific goal that is to be achieved. This is, however, not the situation for general control forces. If the influence of the control is not additive, convergent regions depend on the applied forces, i.e., the eigenvalues of $Df_z^{(n)}$ at $\mathbf{z}^{(n)}$ depend on the next desired goal point, $\mathbf{z}^{(n+1)}$ (which is *a priori* arbitrary). Therefore determination of stable goals becomes a more difficult task. However, we can determine convergent regions for fixed point control,

$$\mathbf{z}^{(n+1)} = \mathbf{z}^{(n)} = \mathbf{z}^*. \tag{16}$$

Then, control forces $\mathbf{F}^*$ are constant in time, depending only on $\mathbf{z}^*$, and eigenvalues of

$$Df_z^* = \left(\frac{\partial f_i}{\partial z_j}\right)\Big|_{\mathbf{z}^*,\mathbf{q},\mathbf{F}^*}, \quad i,j = 1,\ldots,d \tag{17}$$

can be calculated. The locations in phase space where all eigenvalues of Df_z^* have an absolute value less than unity (i.e., where controlled fixed points are asymptotically stable) are called *FP-convergent regions* in the following. They are not independent of the way control forces act on the system, as forces are involved in the Jacobian (17). The (usual) convergent regions are recovered as the special case of FP-convergent regions for additive forces. These regions are not very useful, however, in the case of nonadditive control, because convergent regions and FP-convergent regions may differ significantly.

One can expect that also nonstationary goals can be established within FP-convergent regions if their dynamics is suitably limited. In the case of iterated map dynamics, a sufficient condition is the choice of consecutive goal points $\mathbf{z}^{(n)}$ and $\mathbf{z}^{(n+1)}$ in such a way that the absolute eigenvalues of (10) remain smaller than unity (e.g., the difference $\mathbf{z}^{(n+1)} - \mathbf{z}^{(n)}$ can be kept sufficiently small). If a periodic goal of period N is considered, the eigenvalues of the product of Jacobians along the goal orbit

$$\prod_{n=0}^{N-1} Df_{\mathbf{z}}^{(n)} = \prod_{n=0}^{N-1} \left(\frac{\partial f_i}{\partial z_j}\right)\Big|_{\mathbf{z}^{(n)},\mathbf{q},\mathbf{F}^{(n)}} \tag{18}$$

should have an absolute value smaller than unity to ensure stability.

Dynamic goals need not be restricted to FP-convergent regions, as the areas where nearby orbits converge are altered by the applied forces (which depend on the dynamics of the goal) and thus are dynamic themselves. However, for "slowing down" the goals, i.e., reducing the distances $\mathbf{z}^{(n+1)} - \mathbf{z}^{(n)}$ more and more, they converge to the (stationary) FP-convergent regions. A calculation of FP-convergent regions is therefore also helpful to estimate the areas where parametric entrainment control is applicable for dynamic goals. This is used in some of the examples.

While a detailed investigation of the problem of stability and also of the extensions of basins might prove to be even more involved than in the special case of additive forces (see Refs. [45,46,49]), dynamic convergent regions might also exhibit new possibilities for entrainment control. This should be addressed in a subsequent investigation.

To include a modeling error in our considerations, we permit a nonvanishing second term on the right hand side of Eq. (12). This leads to a systematic deviation of the actual dynamics from the desired one. However, if $|\mathbf{p}-\mathbf{q}|$ is small enough, the parameter error does not change the eigenvalues of the Jacobians too much, and we do not expect a great effect on stability of our (now shifted) goal. The systematic shift can be used to apply the above mentioned general resonance spectroscopy to the experimental system [55].

Returning to Eq. (7), different cases of solvability may occur in general. In the following we suppose that unique solutions of this set of d nonlinear equations exist. Other cases (none or nonunique solutions) are briefly discussed in Sec. V.

A simplification arises if the control acts in such a way that all partial derivatives of the map with respect to the forces vanish except for first order, i.e., $\partial^l f_i/\partial F_j^l \equiv 0, l \geq 2$. Then we can linearize

$$\mathbf{f}(\mathbf{z}^{(n)},\mathbf{q},\mathbf{F}^{(n)}) = \mathbf{f}(\mathbf{z}^{(n)},\mathbf{q},\mathbf{0}) + Df_F^{(n)}\mathbf{F}^{(n)} \tag{19}$$

with the help of the Jacobi matrix evaluated at zero control forces:

$$Df_F^{(n)} = \left(\frac{\partial f_i}{\partial F_j}\right)\Big|_{\mathbf{z}^{(n)},\mathbf{q},\mathbf{0}}, \; i=1,\ldots,d\,,\; j=1,\ldots,s. \tag{20}$$

If the Jacobi matrix is invertible, we can solve Eq. (7) directly for the control forces

$$\mathbf{F}^{(n)} = \left[Df_F^{(n)}\right]^{-1}\left[\mathbf{g}(\mathbf{z}^{(n)}) - \mathbf{f}(\mathbf{z}^{(n)},\mathbf{q},\mathbf{0})\right]. \tag{21}$$

The form of this equation resembles the case of additive forces (compare Ref. [43]) except for the multiplication with the inverse Jacobian. Note that the Jacobian changes each time step, and that complications occur if no inverse exists, especially if $d \neq s$ (see Sec. V).

In the general situation where higher order derivatives with respect to the control forces appear, the linearization Eq. (19) can be considered as the first step of a Newton iteration scheme to solve Eq. (7). It might be necessary to proceed with the iteration to gain sufficiently exact control.

III. ITERATED MAP DYNAMICS

As a first, quite simple example we consider the parametrically controlled logistic map

$$x^{(n+1)} = (\lambda + F^{(n)})x^{(n)}(1-x^{(n)}), \quad x \in [0,1], \lambda \in [0,4]. \tag{22}$$

The control, added to the multiplicative parameter, acts linearly [i.e., the linearization (19) is exact], but is not additive. Equation (22) should be the "experimental" system, and our "model" equation differs only by the parameter, called $\tilde{\lambda}$ instead of λ:

$$y^{(n+1)} = (\tilde{\lambda} + F^{(n)})y^{(n)}(1-y^{(n)}). \tag{23}$$

Equations (7) and (12) yield the control forces

$$F^{(n)} = z^{(n+1)}/[z^{(n)}(1-z^{(n)})] - \tilde{\lambda} \tag{24}$$

and the linearization

$$x^{(n+1)} - z^{(n+1)} = (\tilde{\lambda} + F^{(n)})(1-2z^{(n)})(x^{(n)} - z^{(n)}) + z^{(n)}(1-z^{(n)})(\lambda - \tilde{\lambda}), \tag{25}$$

respectively. The (one-dimensional) Jacobi matrix reads

$$\left.\frac{df}{dz}\right|_{z^{(n)},\tilde{\lambda},F^{(n)}} = (\tilde{\lambda} + F^{(n)})(1-2z^{(n)}) = \frac{z^{(n+1)}(1-2z^{(n)})}{z^{(n)}(1-z^{(n)})}. \tag{26}$$

Here the control force $F^{(n)}$ could be substituted by its analytical expression which leads to the occurrence of both $z^{(n)}$ and $z^{(n+1)}$. If we consider a fixed point z^* to be stabilized [Eq. (16)], we find that every fixed point in the interval $[0, \frac{2}{3}]$ is a stable goal. It turns out that the fixed point control force simply tunes the parameter to a value where the stable fixed point is the natural dynamics of the logistic map. Indeed, this is only possible for points within the above interval, corresponding to controlled parameter values $(\lambda + F) \in [1,3]$. Although the fixed point control is trivial, the control of a dynamic goal is not, since it does *not* simply consist of chained fixed point controls.

From Eqs. (24) and (25), we calculate a systematic displacement of a controlled fixed point $x^{(\infty)}$ which depends on the deviation of our model parameter from the experimental value, according to

$$x^{(\infty)} - z^* = (1-z^*)^2(\lambda - \tilde{\lambda}). \tag{27}$$

The displacement can be used for an accurate determination of the system parameter λ (compare Ref. [55]). For a chaotic logistic map ($\lambda = 3.8$) which is driven to a fixed point $z^* = 0.5$, we show, in Fig. 1, the mean distance of experiment and goal,

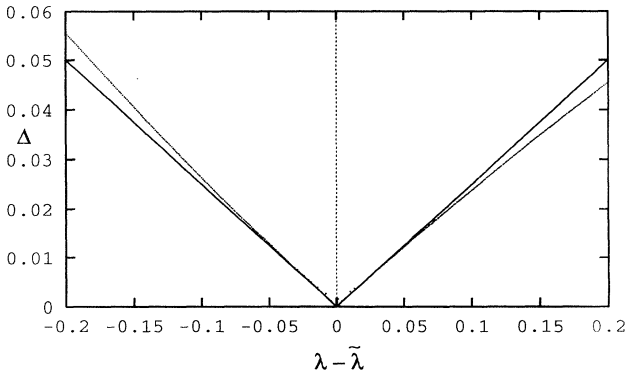

FIG. 1. Mean distance Δ of experimental fixed point and goal fixed point for a parametrically controlled logistic map (dots). $\lambda - \tilde{\lambda}$ gives the distance between experimental and model parameters. The theoretical linear dependence is given by the solid line.

$$\Delta = \langle |x^{(n)} - z^{(n)}| \rangle, \tag{28}$$

which is plotted vs detuning of experiment and model parameter. The theoretical values according to Eq. (27), valid for small $\lambda - \tilde{\lambda}$, are given by the solid line. The parameter of the experiment can be determined with high precision by tracking the matching of the controlled and the actually desired fixed point.

The most conservative stability estimation for a dynamic goal, considering a goal dynamics of points jumping arbitrarily within the unit interval, leads to stable goals within the interval $[(3-\sqrt{5})/2, (\sqrt{5}-1)/2]$. To demonstrate that the goal trajectory indeed may be arbitrary within this region, Fig. 2 shows the control of a chaotic logistic map which leads first to a period-three goal and second to another chaotic goal trajectory, restricted to the stable interval. The model parameter is chosen slightly different than the experiment's parameter ($\lambda = 3.9$, $\tilde{\lambda} = 3.8$), which leads to small systematic displacement of system and goal dynamics. However, this does not hinder the emergence of the goal, although the near-entrained dynamics is shifted slightly across the upper interval boundary. Note that the system, when controlled, is no longer "chaotic" in the sense of sensitive dependence on initial conditions (positive Lyapunov exponent), but is entrained to one specific aperiodic orbit (that has been generated before by another chaotic logistic map, suitably transformed to be located within the stable interval).

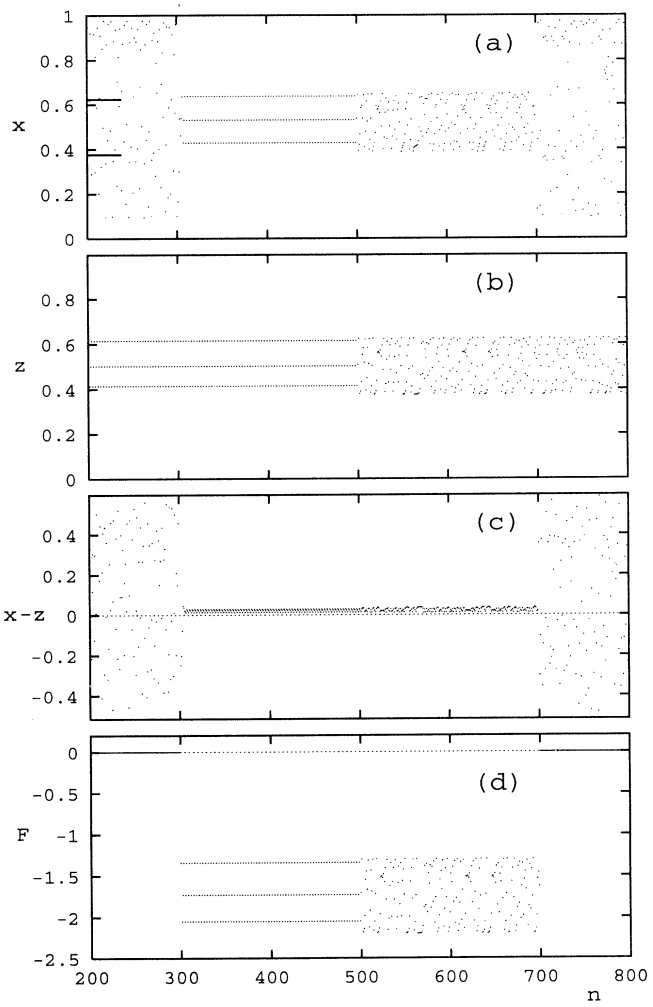

FIG. 2. Parametric control of the logistic map Eq. (22), $\lambda = 3.9$, $\tilde{\lambda} = 3.8$. The abscissa denotes the iteration number n. Control for a period-3 goal is turned on at $n = 300$, switched to an aperiodic goal at $n = 500$, and turned off at $n = 700$. (a) Orbit $x^{(n)}$ of the controlled system. The long bars at the ordinate indicate the estimated region of stable entrainment for arbitrary control. (b) Goal dynamics $z^{(n)}$. (c) Deviation $x^{(n)} - z^{(n)}$ of system from goal dynamics. (d) Control force $F^{(n)}$.

The next example considers higher dimension as well as a more complicated influence of the control. It is carried out for the Hénon map. The experimental system is the following:

$$\begin{aligned} x_1^{(n+1)} &= e^{F_2^{(n)}} + x_2^{(n)} - (a + F_1^{(n)})(x_1^{(n)})^2, \\ x_2^{(n+1)} &= (b + F_2^{(n)}) x_1^{(n)} + F_1^{(n)}. \end{aligned} \tag{29}$$

We have two forces to control the two-dimensional system, but both forces influence both variables. Additionally, the influence of F_2 is nonlinear. Here, this leads to the need for numerical calculation of the forces by solving Eq. (7). This has been done by a Newton iteration scheme. Our "model" of the system differs in the values of the parameters, $\tilde{a}$ and $\tilde{b}$ instead of a and b; we set $a = 1.4$, $b = 0.3$ and $\tilde{a} = 1.45$, $\tilde{b} = 0.25$. The regions where stable fixed point control is possible (the FP-convergent regions) have been calculated using the eigenvalues of the matrix (17), and are given as gray areas in Fig. 3 (note the difference to the convergent region for additive forces, given in Ref. [49]). The unperturbed Hénon attractor (i.e., $a = 1.4$, $b = 0.3$, and $F_1^{(n)} = 0 = F_2^{(n)}$) is also plotted as an orientation in

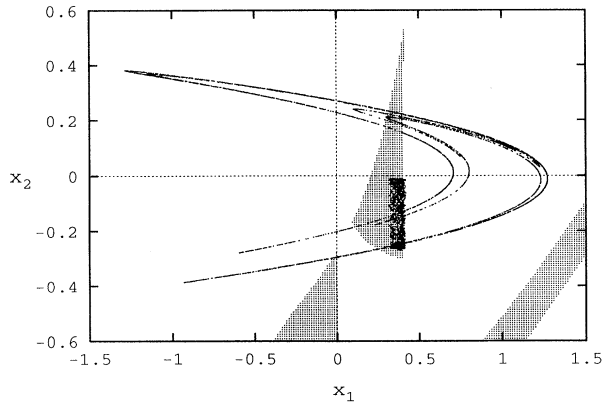

FIG. 3. Phase plane of the Hénon system Eq. (29). The uncontrolled attractor for $a = 1.4$, $b = 0.3$ is visible as well as an aperiodic goal attractor, forming the dark rectangle. The gray areas indicate the FP-convergent regions.

the variable plane. Our goals are chosen to lie (mainly) within the indicated FP-convergent regions. Figure 4 shows applied control to the above Hénon map Eq. (29). Fixed point, period-three, and aperiodic ("chaotic") dynamics are achieved in the given example. The deviation of the experiment from the goal is measured with the norm $\delta = \sqrt{(x_1 - z_1)^2 + (x_2 - z_2)^2}$. Because of slightly "wrong" model parameters, we again see a systematic shift of the goal dynamics. However, for identical parameter values of experiment and model, the deviation would approach zero. The location of the "chaotic" goal attractor in the x_1-x_2 plane is also given in Fig. 3 (the darker "fuzzy" rectangle). It corresponds to the dynamics of two uncoupled chaotic logistic maps, one in each coordinate. Note that this goal has also small parts lying outside the FP-convergent regions.

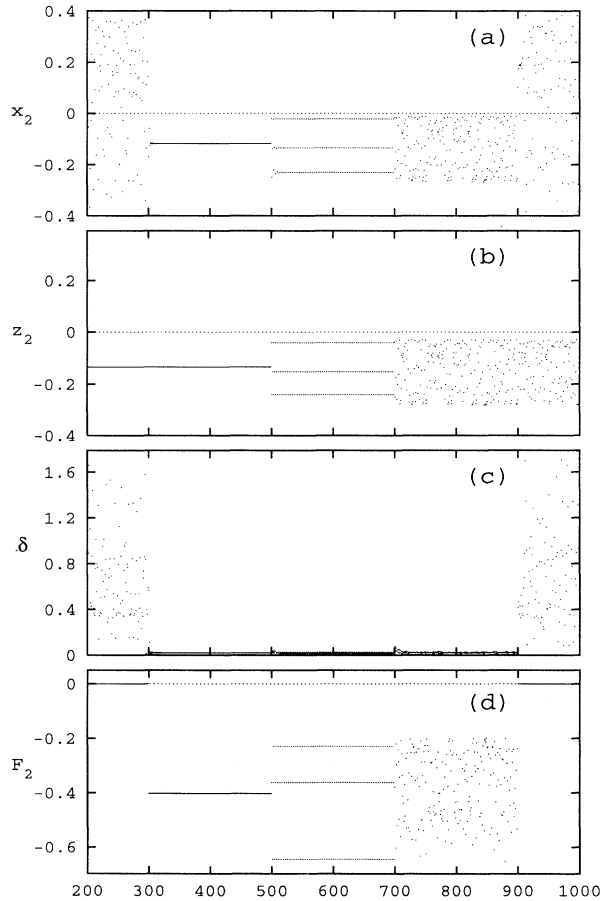

FIG. 4. Parametric control of the Hénon system Eq. (29), $a = 1.4$, $b = 0.3$, $\tilde{a} = 1.45$, $\tilde{b} = 0.25$. The abscissa denotes the iteration number n. Control for a period-1 goal is turned on at $n = 300$, switched to a period-3 goal at $n = 500$, switched again to the aperiodic goal shown in Fig. 3 at $n = 700$, and turned off at $n = 900$. (a) Orbit of the second system variable $x_2^{(n)}$. (b) Second goal variable $z_2^{(n)}$. (c) Deviation δ between system and goal (see text). (d) Second control force $F_2^{(n)}$.

IV. ORDINARY DIFFERENTIAL EQUATIONS

The expansion of the control technique to continuous systems (ODEs) instead of difference equations is straightforward: just replace $\mathbf{x}^{(n)}$ and $\mathbf{z}^{(n)}$ by $\mathbf{x}(t)$ and $\mathbf{z}(t)$, $\mathbf{x}^{(n+1)}$ and $\mathbf{z}^{(n+1)}$ by $\dot{\mathbf{x}}(t)$ and $\dot{\mathbf{z}}(t)$, and $\mathbf{F}^{(n)}$ by $\mathbf{F}(t)$, where dots denote time derivatives. The replacements lead to the continuous analog of Eq. (7):

$$\mathbf{f}(\mathbf{z}(t), \mathbf{q}, \mathbf{F}(t)) = \mathbf{g}(\mathbf{z}(t)) = \dot{\mathbf{z}}(t). \tag{30}$$

Equation (12) turns into

$$\dot{\mathbf{x}}(t) - \dot{\mathbf{z}}(t) = Df_z(t)\,[\mathbf{x}(t) - \mathbf{z}(t)] + Df_q(t)(\mathbf{p} - \mathbf{q}). \tag{31}$$

The FP-convergent criterion changes to negative real parts of the eigenvalues of the Jacobian Df_z^* [Eq. (17)], evaluated at points $\mathbf{z}^*$ and forces $\mathbf{F}^*$ according to

$$\mathbf{f}(\mathbf{z}^*, \mathbf{q}, \mathbf{F}^*) = \mathbf{0}. \tag{32}$$

Fixed point goals are asymptotically stable in the FP-convergent regions, but statements about stability of dynamic goals are more difficult to make than in the discrete dynamics case: Even for additive control, dynamic goals, albeit entirely located within convergent regions, need not be stable if they are not suitably dynamically limited (i.e., they do not change "too rapidly" [48]). Usually, for individual goals a stability analysis has to be carried out, employing well known but lengthy techniques (like Floquet theory for periodic goals). Again, FP-convergent regions give us a useful hint about where to try entrainment control with dynamic goals, but a general statement about arbitrary goals is obviously not possible. As a rough estimate, the goal trajectory $\mathbf{z}(t)$ should not behave faster than a typical relaxation to a fixed point goal within the considered FP-convergent region:

$$\frac{\max_t \|\dot{\mathbf{z}}(t)\|}{\max_{t_1,t_2} \|\mathbf{z}(t_1) - \mathbf{z}(t_2)\|} < \max_t \hat{\mu}_r^*(\mathbf{z}(t)). \tag{33}$$

$\hat{\mu}_r^*(\mathbf{z}(t))$ denotes the largest (negative) real part of the eigenvalues of matrix (17) at $\mathbf{z}^* = \mathbf{z}(t)$. However, this estimate, based on local convergence all along the goal trajectory, might prove to be too conservative, since it is known that stable nonstationary solutions can pass regions without local convergence (e.g., the limit cycle of the van der Pol equation). Thus we consider the mean local convergence along a periodic goal trajectory as another estimate for stability:

$$\bar{\mu}_r = \langle \hat{\mu}_r(\mathbf{z}(t), \dot{\mathbf{z}}(t)) \rangle = \frac{1}{T} \int_0^T \hat{\mu}_r(\mathbf{z}(t), \dot{\mathbf{z}}(t)) dt, \tag{34}$$

where T denotes the period of the goal. Note that here, in contrast to Eq. (33), the largest real part of the eigenvalues of the Jacobian $Df_z(t)$ with correct forces $\mathbf{F}(t)$ [according to Eq. (30)] is used, denoted by $\hat{\mu}_r$. This quantity depends on $\dot{\mathbf{z}}(t)$ and can be positive. A negative mean $\bar{\mu}_r$, however, should point to stability of the goal.

As a first example of a differential equation, we consider the Lorenz system [58], which is parametrically con-

trolled:

$$\begin{aligned}\dot{x}_1 &= (\sigma + F_1)(x_2 - x_1),\\ \dot{x}_2 &= (r + F_2)x_1 - x_2 - x_1 x_3,\\ \dot{x}_3 &= x_1 x_2 - (b + F_3)x_3.\end{aligned} \tag{35}$$

Because the control forces act on multiplicative parameters, control is linear in this case and Eq. (21), changed to the continuous analog, is valid. Correct forces can be determined analytically for each given goal location (z_1, z_2, z_3) and derivative $(\dot{z}_1, \dot{z}_2, \dot{z}_3)$:

$$\begin{aligned}F_1 &= \frac{\dot{z}_1}{z_2 - z_1} - \sigma,\\ F_2 &= \frac{\dot{z}_2 + z_2 + z_1 z_3}{z_1} - r,\\ F_3 &= \frac{-\dot{z}_3 + z_1 z_2}{z_3} - b.\end{aligned} \tag{36}$$

One notes that divergent forces appear if the goal crosses one of the planes $x_1 = x_2$, $x_1 = 0$, or $x_3 = 0$. Also, the goals [as all solutions of Eq. (35)] are degenerate in the sense that the plane-mirrored trajectory $x_1(t) \to -x_1(t)$, $x_2(t) \to -x_2(t)$, $x_3(t) \to x_3(t)$ is also valid. Therefore nonsymmetric goals may show up in their reflected variant, depending on the system state when control starts. Additionally it turns out, when calculating the eigenvalues of the Jacobian Df_z^* for the search of FP-convergent regions, that each controlled fixed point possesses an indifferent direction in phase space with zero eigenvalue. This corresponds to a further degeneracy of controlled fixed points: In the case of perfectly matching model parameters, there exists a one-dimensional set of other fixed points in phase space with identical control forces. This happens because F_1 is always set to $-\sigma$, irrespective of the fixed point coordinates, which leads to a nonuniqueness of controlled fixed points. However, this kind of degeneracy is removed if the model parameters differ from the exact values, and also in the case of nonstationary goals ($\dot{\mathbf{z}} \not\equiv 0$). A calculation of "semi-FP-convergent" regions (permitting eigenvalues to have zero real part) as a hint for regions of stable goals therefore seems to be justified. In a plane of constant third coordinate ($x_3 = 25.0$), Fig. 5 shows the region where controlled fixed points are stable in the sense that besides the zero eigenvalue the other two have negative real part (gray area).

As a periodic goal, we choose a harmonic oscillation located within the indicated plane and the semi-FP-convergent region: $z_1(t) = 4\cos(\omega t) + 10$, $z_2(t) = -12\sin(\omega t) + 12$, $z_3 = 25$. To estimate a frequency ω suitable for stability of our goal, obviously our first approach, Eq. (33), cannot be employed, since the largest eigenvalue for fixed point control is always zero. However, a calculation following Eq. (34) results in negative means $\bar{\mu}_r(\omega)$ in the frequency range $\omega \in (0, 17]$. A minimum of $\bar{\mu}_r$ appears at $\omega \approx 4$. The Lorenz system can indeed successfully be controlled to the harmonic goal with $\omega = 3.0$, as is shown by the trajectory plotted in Fig. 5 (projected onto the plane $x_3 = 25.0$). The actual desired goal trajectory is given by the dashed ellipse in the first quadrant. The system parameters of $\sigma = 9.8$, $r = 27.0$, and $b = 2.7$ were slightly different from the model parameters $\tilde{\sigma} = 10.0$, $\tilde{r} = 28.0$, and $\tilde{b} = 2.6666$ that were used to calculate forces. Obviously, the periodic solution on which the system is trapped shows only a small distortion from the actual goal limit cycle (also in the x_3 direction, which is not visible here). Time plots of the second coordinates of system and goal, $x_2(t)$ and $z_2(t)$, and the first control force $F_1(t)$ are given in Fig. 6. Control is switched on at $t = 30.0$ and turned off again at $t = 65.0$. After a short transient, the system entrains to the periodic goal, which is left immediately after control.

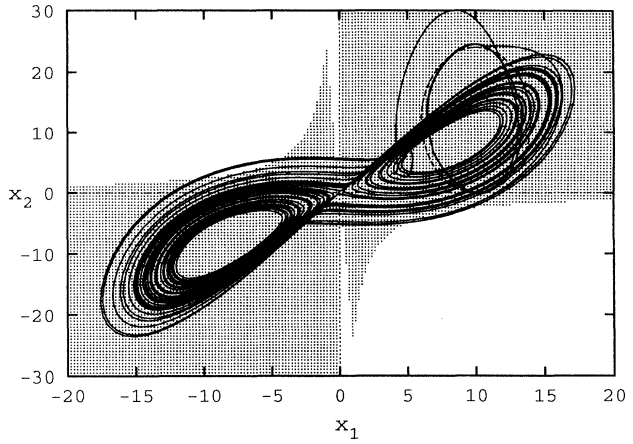

FIG. 5. Projection of the Lorenz system Eq. (35) onto the plane $x_3 = 25.0$. Semi-FP-convergent regions (see text) are indicated by the gray area. The chaotic Lorenz attractor ($\sigma = 9.8$, $r = 27.0$, $b = 2.7$) is driven by control to a periodic movement near the goal (dashed ellipse) which is located within this plane ($x_3 = 25.0$). The trajectory corresponds to Fig. 6.

The control force F_1, which in the ideal case becomes singular [for isolated times $z_1(t) = z_2(t)$], has been limited by a restriction to the interval $[-15, -2]$. Obviously, neither the sudden jump of the force nor its truncation at finite values results in a loss of control in the example. Strictly speaking, however, the *exact* goal trajectory can no longer be a solution of the controlled equation, even for exact modeling parameters. Therefore near entrainment actually takes place.

We examined the total frequency range of negative $\bar{\mu}_r(\omega)$ (for control signals calculated with the true parameters). This revealed that the Lorenz system could be near entrained for goal frequencies in the approximate interval $\omega \in [2, 6]$, which is close to the minimum at $\omega \approx 4$. In the remaining area, entrainment to a periodic solution also took place, but the distances to the desired goal became more significant ("far entrainment"), and additional effects such as period doubling and transient beat oscillations appear. These phenomena seem to be due to the extension of nonattracting parts of the goal for larger $\bar{\mu}_r$, combined with the at times (almost) singular control forces. (Because the chaotic system becomes regular apart from the goal trajectory in these cases, one rec-

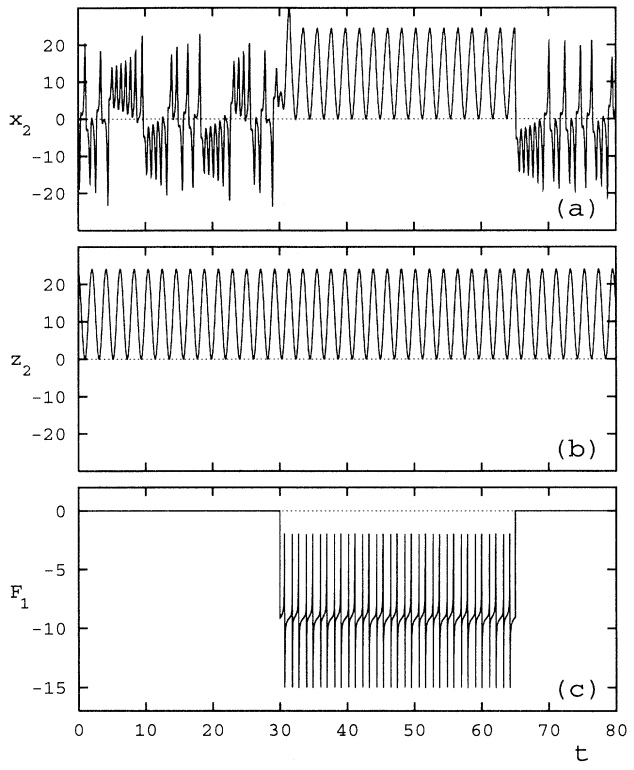

FIG. 6. The same control as used in Fig. 5. The abscissa denotes the dimensionless time t. Control is turned on at $t = 30.0$ and turned off at $t = 65.0$. (a) Second system variable $x_2(t)$. (b) Second goal variable $z_2(t)$. (c) Control force $F_1(t)$. The spikes correspond to divergences which are truncated suitably.

ognizes similarities to the suppression of chaos by other periodic perturbation methods without any goal [32–42].)

Larger distortions appear also for goals reaching slightly outside the FP-convergent area and for larger differences of system and model parameters. As expected, we also find entrainment to mirrored goals, depending on initial conditions. Let us note that entrainment to aperiodic goals (which is not shown here) works, too, supposing the goal dynamics is sufficiently slow and takes place mainly in FP-convergent regions.

In the following, we briefly want to demonstrate the spectroscopic method described above [55], using parametric control of an ODE. We take a three-dimensional system that is known in the literature as the three-variable autocatalator (TVA). It models a chemical reaction of a precursor reactant to a final product via three intermediate species. For certain parameter choices, the equations exhibit period doubling and chaotic behavior [57]. In our spectroscopic approach, we introduce three control forces for open-loop control: One force changes the concentration of the precursor species (affecting the variable μ), and two other controls add to the time derivatives of the concentrations of the intermediate reactants, dx_2/dt and dx_3/dt, respectively. This leads to the equations

$$\begin{aligned}\dot{x}_1 &= \mu(1+F_1)(\kappa+x_3) - x_1(1+x_2^2),\\ \dot{x}_2 &= \frac{1}{\sigma}[x_1(1+x_2^2) - x_2] + F_2,\\ \dot{x}_3 &= \frac{1}{\delta}(x_2 - x_3) + F_3.\end{aligned} \tag{37}$$

F_1 is introduced in such a way that it directly gives the fraction of the parameter μ that is changed. Note that the influence of F_2 and F_3 on the derivatives models added *flows* of the intermediate chemicals into the process, while F_1 provides (possibly fast) switches of the precursor *concentration*, which is an integrated flow rate. Therefore large precursor flows would possibly be necessary in a real experiment. Note also that the variables and parameters are rescaled to be dimensionless, see [57]. As in the Lorenz system above, the equations can be solved directly for the needed control forces if a specific goal dynamics is given.

The parameter values of the controlled system (the "experiment") were set to $(\mu,\kappa,\sigma,\delta) = (0.152, 70, 0.0045, 0.025)$ which leads to chaotic behavior. In the following, system parameters σ and δ are determined by trying to stabilize the system to a fixed point and by checking deviations from the desired stationary state [55]. Figure 7(a) shows the chaotic attractor of Eq. (37) and the approximate location of the controlled fixed point, $(x_1^*, x_2^*, x_3^*) = (0.06, 15.0, 17.0)$, indicated by the arrow. This point turns out to be controllable with quite small control forces: For exactly matching model parameters, we find $F_1 = 0.0254, F_2 = 320.0, F_3 = 80.0$, and typical values of $\dot{x}_2$ and $\dot{x}_3$ on the chaotic attractor are orders of magnitude larger than F_2 and F_3. A typical time behavior of the controlled system, represented by the concentration $x_1(t)$, is shown in Fig. 7(b): After switching on the control forces (at $t = 1.0$) the system settles down quite rapidly to a fixed point in phase space, and after turning off control (at $t = 2.0$), the chaotic movements resume. The better the modeling parameters for calculating forces, the less the fixed point is shifted from its intended position. In this case of fixed point control, we can define a resonance or response function

$$R = (|\mathbf{x}^f - \mathbf{z}^*|)^{-1}, \tag{38}$$

where $\mathbf{z}^*$ denotes the desired fixed point and $\mathbf{x}^f$ is the final steady state of the system after some time of control. In order to maximize R, parameters of the model equation (and therefore the control forces) are varied over a reasonable area. The result of simulation of this form of spectroscopy is shown in Fig. 7(c), where R is plotted vs. the reaction parameters $\tilde{\sigma}$ and $\tilde{\delta}$ that had been used in the model ($\tilde{\mu} = \mu$, $\tilde{\kappa} = \kappa$). A response maximum appears where the model parameters match the values of the experiment. This method of resonance spectroscopy is, of course, not restricted to originally chaotic systems. However, we show here that it is applicable irrespective of complicated phase space structures if an appropriate model is available.

In an application, restrictions such as too few control forces or limited control strength may exist. In the following example we show that even in these cases a model-

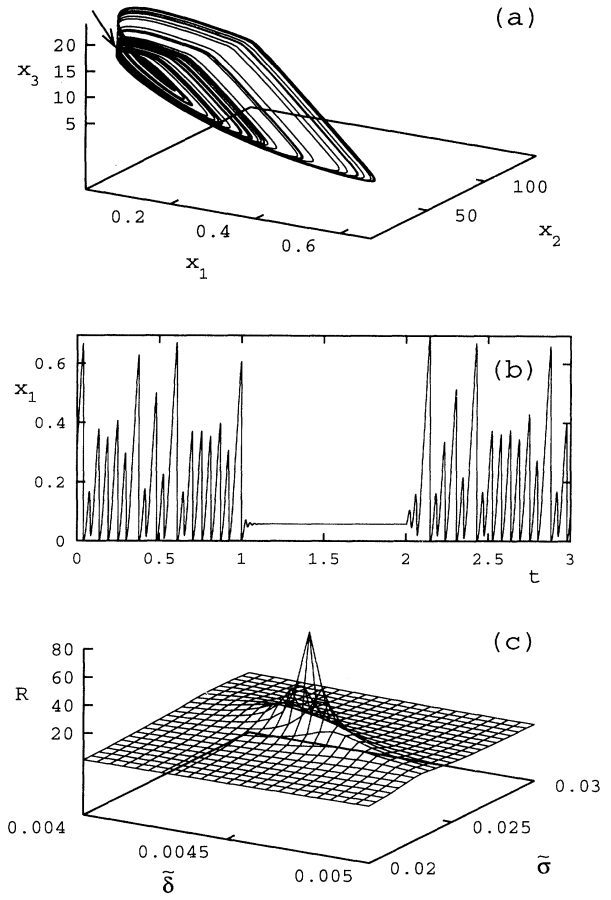

FIG. 7. Control and generalized resonance spectroscopy of the TVA system Eq. (37) (see text for parameter values). (a) Chaotic attractor of the uncontrolled system. The arrow indicates the position of the fixed point used for spectroscopy by the control. (b) First variable $x_1(t)$ of the system driven to the fixed point. Control is turned on at the dimensionless time $t = 1.0$ and off at $t = 2.0$. (c) Response function R [Eq. (38)] vs modeling parameters $\tilde{\delta}$ and $\tilde{\sigma}$. Maximum response (best match of observed and desired fixed point) is shown for the true system parameters, $\delta = 0.0045$ and $\sigma = 0.025$ (the value of R actually tends to infinity for exact matching parameters and is cut off in the plot).

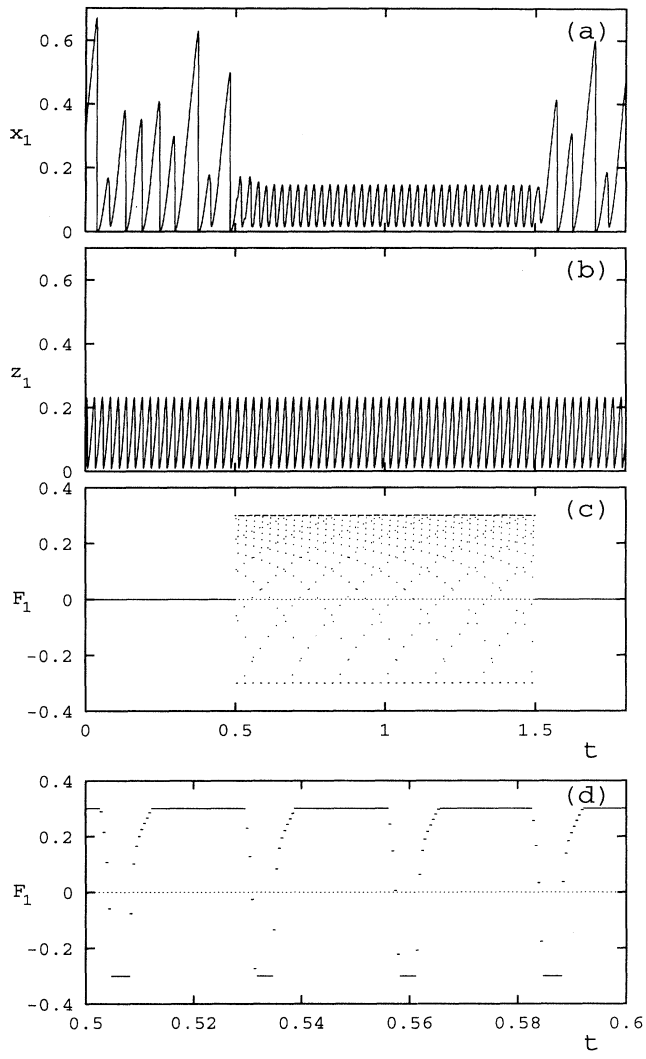

FIG. 8. Control of the TVA system Eq. (37) with restricted control forces: Only the first (parametrically acting) force F_1 is applied. The abscissa denotes the dimensionless time t. Control is active from $t = 0.5$ to $t = 1.5$. The goal, a limit cycle, is not attainable, but a similar movement sets in. (a) First system variable $x_1(t)$. (b) First goal variable $z_1(t)$ (note the larger amplitude). (c) Parametric control force F_1. It has been applied as a ("digital") staircase function and limited to values up to ± 0.3 (see text). (d) Enlargement of the time scale of (c).

based aproach can be advantageous and lead to entrained behavior. Additionally, we simulate digital control (compare Ref. [59]), i.e., the control forces are not given as a continuous function, but as a staircase function (the forces are held constant for a certain time interval Δt). This case is met, e.g., in experiments where change of control forces is restricted to some smallest time interval. The applied control appears as a more or less good approximation of the theoretical shape. One should expect difficulties for entrainment if Δt is not sufficiently small.

Figure 8 shows a restricted control of the TVA system Eq. (37). The first coordinate of controlled system and goal, $x_1(t)$ and $z_1(t)$, and the control force $F_1(t)$ are plotted vs the same time axis in Figs. 8(a)–8(c). As a goal trajectory we use a limit cycle that is an attractor of the system for the parameter set $(\mu, \kappa, \sigma, \delta) = (0.160, 65, 0.005, 0.02)$, but which we have accelerated in speed by a factor 1.66. The parameters of the "experiment" have been set again to the values $(\mu, \kappa, \sigma, \delta) = (0.152, 70, 0.0045, 0.025)$ for a chaotic state. Control forces have been calculated with model parameters $(\tilde{\mu}, \tilde{\kappa}, \tilde{\sigma}, \tilde{\delta}) = (0.154, 65, 0.005, 0.02)$ and according to Eq. (37), i.e., with the assumption that all three forces exist. However, for control only the parametric force F_1

is used. Additionally, the values of F_1 are restricted to a change of the parameter μ of $\pm 30\%$, so the force is bounded to the interval $[-0.3, 0.3]$ (values are set onto the boundaries where they would exceed them). The resulting shape of F_1 is given in Fig. 8(c) and, on an expanded time scale, in Fig. 8(d). One recognizes the short time intervals where the force is held constant ($\Delta t = 0.0005$). Within some periods the force is in upper or lower saturation. The control is applied from $t = 0.5$ to $t = 1.5$, and indeed the system settles down onto a limit cycle. Note that this controlled limit cycle is not exactly the goal trajectory for it has a significantly smaller amplitude. It appears that this deviation is neither due to incomplete, cut off, or discretized control forces, nor to inexact modeling parameters, but has possibly some deeper reason. We checked this example, and the exact goal turned out to be unstable, even if all three forces were applied correctly. However, the system did not return to chaotic behavior after leaving the unstable goal, but switched to a different limit cycle of the same period and smaller amplitude, very similar to our imperfectly controlled system (Fig. 8). Therefore our control forces introduced both an unstable goal solution and a stable solution that is similar to the goal in certain aspects. A similar solution still exists in the imperfectly controlled case. This is no example of a near entrainment as described above, because the dynamics is not just the distorted goal, and it cannot be used for spectroscopic purposes. However, we still have a far-entrained solution which removes chaos. This phenomenon of controlled system behavior that does not follow (near to) the goal, but nevertheless acts in a synchronized manner, occurred for several parameters and systems, and also for aperiodic goals. It might be a more universal feature of parametrically controlled systems and should be compared to effects of other parametric perturbation methods. Referring to our TVA example (Fig. 8), however, let us note that the model-based character of the control force F_1 is important. Several attempts to entrain the system with more simple control forces of the same frequency and the same maximum amplitude (such as sinusoidal or square wavelike signals) did not work. Although the TVA behavior changed significantly in these cases, chaos could not be suppressed.

V. SUMMARY AND OUTLOOK

We have shown that the idea of an extended model-based entrainment control, including parametric control forces, can successfully be applied to chaotic systems. The method has been investigated for nonadditive control of discrete dynamics (logistic and Hénon map) and continuous-time systems (Lorenz and TVA equations). A generalization of the concept of convergent regions (FP-convergent regions) has been introduced and proves to be useful for determination of stable goal dynamics. Quantitative estimates for dynamical limitations of goals have been given, while a strict treatment of the stability problem for a larger variety of goal dynamics remains a challenging and difficult task. Nevertheless, parametric entrainment control might open new possibilities, as *control of convergent regions* of a system could be developed in future work.

Moreover, we have demonstrated that generalized resonance spectroscopy as described in Ref. [55] can easily be applied to parametrically controlled systems, both iterated maps and ODEs. This aspect includes the fact that model-based parametric control forces may show a certain amount of robustness against deviations of experiment and model. Also, incomplete access and restricted values of the forces are problems that do not necessarily hinder control (in contrast, system dynamics can be more sensitive to parametric disturbance than to, e.g., additive forcing, which might balance out the lack of control access in some cases). Furthermore, a model-based derivation of (in this case parametric) control forces should be superior to application of more simple periodic system perturbations. In particular, harmonic forces [32–36,41,42] reject many degrees of freedom of the control (higher modes) that might be useful [37–40,60]. The exact relationship, however, of model-based parametric entrainment control to former approaches, like the other periodic perturbation methods cited, still has to be clarified, as similar effects may appear for inexact forces and unstable goals.

Due to experimental constraints, limitations in magnitude of control forces are often given which restrict the goal dynamics that are accessible. In addition to these "limited value" restrictions, the problem of solvability of the control force equations (7) or (30) might occur in the general case of nonadditive forces. In our examples of parametric dependences this appeared as divergences of control forces which were, however, isolated and could be truncated without losing control. If the control influence is more complicated, this problem may become more severe and may exclude many goals. Similar difficulties appear if too few control forces are available or not all components of the system are affected: then a suitable deformation of the system may not be possible by the control. However, one could think of taking the "best" reachable values of control forces by using some optimization process. For example, a pseudoinverse of the Jacobi matrix (20) could be generated using singular value decomposition to "solve" Eq. (21) in a minimum norm sense. Especially with parametric control, an inexact but approximate control might lead to a dynamics similar or synchronized to that desired (compare the last TVA example). The extension of this idea would be to relax the demands on the goal dynamics and to exploit the possibilities of the given control influence with respect to less specific aims. In many cases, the exact goal trajectory is not of really great importance, but other features such as reduction of Lyapunov exponents or a change of correlation functions are actually desired. This would open up a whole area of new goal definitions, circumventing restrictions that might appear in the general case of arbitrary control influence on nonlinear systems. Still, a model-based approach using constrained, but optimized (in some sense) control seems to be promising, but work in this field has just started.

ACKNOWLEDGMENTS

This research was funded in part by the Beckman Institute at the University of Illinois, Urbana-Champaign. Two of us (R.M. and W.L.) were also supported by the Deutsche Forschungsgemeinschaft (Sonderforschungsbereich 185). A.H. was supported in part by a grant from Toshiba Ltd. to Keio University and by Keio University, Tokyo, Japan. A.S. received support from the U.S. National Science Foundation, Grant No. CHE-93-07549.

[1] T. B. Fowler, IEEE Trans. Autom. Control **34**, 201 (1989).
[2] E. Ott, C. Grebogi, and Y. A. Yorke, Phys. Rev. Lett. **64**, 1196 (1990).
[3] W. L. Ditto, S. N. Rauseo, and M. L. Spano, Phys. Rev. Lett. **65**, 3211 (1990).
[4] U. Dressler and G. Nitsche, Phys. Rev. Lett. **68**, 1 (1992).
[5] B. Hübinger, R. Doerner, and W. Martienssen, Z. Phys. B **90**, 103 (1993).
[6] A. Garfinkel, M. L. Spano, W. L. Ditto, and J. N. Weiss, Science **257**, 1230 (1992).
[7] V. Petrov, V. Gáspár, J. Masere, and K. Showalter, Nature **361**, 240 (1993).
[8] B. Peng, V. Petrov, and K. Showalter, J. Phys. Chem. **95**, 4957 (1991).
[9] E. R. Hunt, Phys. Rev. Lett. **67**, 1953 (1991).
[10] R. Roy, T. W. Murphy, Jr., T. D. Maier, Z. Gills, and E. R. Hunt, Phys. Rev. Lett. **68**, 1259 (1992).
[11] B. Peng, V. Petrov, and K. Showalter, Physica A **188**, 210 (1992).
[12] J. Güémez and M. A. Matías, Phys. Lett. A **181**, 29 (1993).
[13] M. A. Matías and J. Güémez, Phys. Rev. Lett. **72**, 1455 (1994).
[14] J. Singer, Y.-Z. Wang, and H. H. Bau, Phys. Rev. Lett. **66**, 1123 (1991).
[15] K. Pyragas, Phys. Lett. A **170**, 421 (1992).
[16] Zhilin Qu, Gang Hu, and Benkun Ma, Phys. Lett. A **178**, 265 (1993).
[17] T. T. Hartley and F. Mossayebi, Int. J. Bifurcation Chaos **2**, 881 (1992).
[18] R. W. Rollins, P. Parmananda, and P. Sherard, Phys. Rev. E **47**, R780 (1993).
[19] P. Parmananda, P. Sherard, R. W. Rollins, and H. D. Dewald, Phys. Rev. E **47**, R3003 (1993).
[20] T. Shinbrot, E. Ott, C. Grebogi, and J. A. Yorke, Phys. Rev. Lett. **65**, 3215 (1990).
[21] T. Shinbrot, W. Ditto, C. Grebogi, E. Ott, M. Spano, and J. A. Yorke, Phys. Rev. Lett. **68**, 2863 (1992).
[22] I. M. Starobinets and A. S. Pikovsky, Phys. Lett. A **181**, 149 (1993).
[23] J. A. Sepulchre and A. Babloyantz, Phys. Rev. E **48**, 945 (1993).
[24] Hu Gang and He Kaifen, Phys. Rev. Lett. **71**, 3794 (1993).
[25] D. Auerbach, Phys. Rev. Lett. **72**, 1184 (1994).
[26] F. Qin, E. E. Wolf, and H.-C. Chang, Phys. Rev. Lett. **72**, 1459 (1994).
[27] B. A. Huberman and E. Lumer, IEEE Trans. Circuits Syst. **37**, 547 (1990).
[28] S. Sinha, R. Ramaswamy, and J. Subba Rao, Physica D **43**, 118 (1990).
[29] D. Vassiliadis, Physica D **71**, 319 (1994).
[30] R. E. Bellman, J. Bentsman, and S. M. Meerkov, IEEE Trans. Autom. Control, **AC-31**, 710 (1986).
[31] R. E. Bellman, J. Bentsman, and S. M. Meerkov, IEEE Trans. Autom. Control, **AC-31**, 717 (1986).
[32] V. V. Alekseev and A. Yu. Loskutov, Dokl. Akad. Nauk. SSSR **293**, 1346 (1987) [Sov. Phys. Dokl. **32**, 270 (1987)].
[33] R. Lima and M. Pettini, Phys. Rev. A **41**, 726 (1989).
[34] A. Azevedo and S. M. Rezende, Phys. Rev. Lett. **66**, 1342 (1991).
[35] Y. Braiman and I. Goldhirsch, Phys. Rev. Lett. **66**, 2545 (1991).
[36] L. Fronzoni, M. Giocondo, and M. Pettini, Phys. Rev. A **43**, 6483 (1991).
[37] M. Salerno, Phys. Rev. B **44**, 2720 (1991).
[38] D. Farrelly and J. A. Milligan, Phys. Rev. E **47**, R2225 (1993).
[39] G. Cicogna and L. Fronzoni, Phys. Rev. E **47**, 4585 (1993).
[40] R. Chacón and J. Díaz Bejarano, Phys. Rev. Lett. **71**, 3103 (1993).
[41] Y. S. Kivshar, F. Rödelsperger, and H. Benner, Phys. Rev. E **49**, 319 (1994).
[42] Yudong Liu and J. R. Rios Leite, Phys. Lett. A **185**, 35 (1994).
[43] A. Hübler and E. Lüscher, Naturwissenschaften **76**, 67 (1989).
[44] B. B. Plapp and A. Hübler, Phys. Rev. Lett. **65**, 2302 (1990).
[45] E. A. Jackson and A. Hübler, Physica D **44**, 407 (1990).
[46] E. A. Jackson, Physica D **50**, 341 (1990).
[47] E. A. Jackson, Phys. Lett. A **151**, 478 (1990).
[48] E. A. Jackson, Phys. Rev. A **44**, 4839 (1991).
[49] E. A. Jackson and A. Kodogeorgiou, Physica D **54**, 253 (1992).
[50] J. L. Breeden, Phys. Lett. A **190**, 264 (1994).
[51] J. L. Breeden and A. Hübler, Phys. Rev. A **42**, 5817 (1990).
[52] J. L. Breeden, F. Dinkelacker, and A. Hübler, Phys. Rev. A **42**, 5827 (1990).
[53] R. Shermer, A. Hübler, and N. Packard, Phys. Rev. A **43**, 5642 (1991).
[54] L. R. Keefe, Phys. Fluids A **5**, 931 (1993).
[55] K. Chang, A. Kodogeorgiou, A. Hübler, and E. A. Jackson, Physica D **51**, 99 (1991).
[56] R. Shermer and M. L. Spano, Proc. SPIE **2037**, 66 (1993).
[57] B. Peng, S. K. Scott, and K. Showalter, J. Phys. Chem. **94**, 5243 (1990).
[58] E. N. Lorenz, J. Atmos. Sci. **20**, 130 (1963).
[59] E. D. Sontag, *Mathematical Control Theory: Deterministic Finite Dimensional Systems* (Springer-Verlag, New York, 1990).
[60] T. Kurz, R. Mettin, A. Kumar, and W. Lauterborn (unpublished).